© 2014. Published by The Company of Biologists Ltd | Development (2014) 141, 2452-2461 doi:10.1242/dev.107797

RESEARCH ARTICLE

A neuron autonomous role for the familial dysautonomia gene *ELP1* in sympathetic and sensory target tissue innervation

Marisa Z. Jackson[1,2], Katherine A. Gruner[1], Charles Qin[1] and Warren G. Tourtellotte[1,2,3,*]

ABSTRACT

Familial dysautonomia (FD) is characterized by severe and progressive sympathetic and sensory neuron loss caused by a highly conserved germline point mutation of the human *ELP1*/*IKBKAP* gene. Elp1 is a subunit of the hetero-hexameric transcriptional elongator complex, but how it functions in disease-vulnerable neurons is unknown. Conditional knockout mice were generated to characterize the role of Elp1 in migration, differentiation and survival of migratory neural crest (NC) progenitors that give rise to sympathetic and sensory neurons. Loss of Elp1 in NC progenitors did not impair their migration, proliferation or survival, but there was a significant impact on post-migratory sensory and sympathetic neuron survival and target tissue innervation. Ablation of Elp1 in post-migratory sympathetic neurons caused highly abnormal target tissue innervation that was correlated with abnormal neurite outgrowth/branching and abnormal cellular distribution of soluble tyrosinated α-tubulin in Elp1-deficient primary sympathetic and sensory neurons. These results indicate that neuron loss and physiologic impairment in FD is not a consequence of abnormal neuron progenitor migration, differentiation or survival. Rather, loss of Elp1 leads to neuron death as a consequence of failed target tissue innervation associated with impairments in cytoskeletal regulation.

KEY WORDS: Elp1, IKBKAP, Familial dysautonomia, Neural crest, Cell migration, Autonomic neuropathy

INTRODUCTION

The hereditary sensory and autonomic neuropathies (HSANs) are a group of neurodevelopmental disorders caused by single gene mutations that give rise to sensory deficits and varying degrees of autonomic dysfunction (Axelrod and Gold-von Simson, 2007; Rotthier et al., 2009; Rotthier et al., 2012). Familial dysautonomia (FD; Riley-Day Syndrome; HSAN3) is the most prevalent HSAN and is characterized by diminished pain and temperature sensation along with progressive autonomic dysfunction (Axelrod, 2004; Axelrod and Gold-von Simson, 2007). Fatality associated with disease is high, with half of patients dying before the age of 40 largely due to autonomic failure (Axelrod, 2004). Although rare within the general population, the autosomal recessive disease has a relatively high carrier frequency in the Ashkenazi Jewish population and an estimated overall incidence of approximately 1/3600 live births (Axelrod, 2004; Lehavi et al., 2003; Maayan et al., 1987).

[1]Department of Pathology (Division of Neuropathology), Feinberg School of Medicine, Northwestern University, 303 E Chicago Ave, Chicago, IL 60611, USA. [2]Northwestern University Integrated Neuroscience (NUIN) Program, Feinberg School of Medicine, Northwestern University, 303 E Chicago Ave, Chicago, IL 60611, USA. [3]Department of Neurology, Feinberg School of Medicine, Northwestern University, 303 E Chicago Ave, Chicago, IL 60611, USA.

*Author for correspondence (warren@northwestern.edu)

Received 7 January 2014; Accepted 16 April 2014

The mutations found to cause FD are all located in the *ELP1*/*IKBKAP* gene with the major haplotype consisting of a noncoding point mutation IVS20+6T>C identified in over 99.5% of individuals with the disease (Anderson et al., 2001; Slaugenhaupt et al., 2001). The mutation is located in the donor splice site of intron 20, which weakens the intron-exon boundary and leads to the variable exclusion of exon 20 from spliced transcripts. Exon 20 skipping introduces a nonsense mutation that gives rise to a truncated Elp1 protein ($Elp1_{Tr}$) that is rapidly degraded (Slaugenhaupt et al., 2001). For poorly understood reasons that may relate to differences in splicing fidelity, the ratio of normal-to-mutant ELP1 mRNA varies across cell types and is particularly low in peripheral sensory and sympathetic neurons in individuals with FD (Cuajungco et al., 2003; Slaugenhaupt et al., 2001). The relatively low levels of Elp1 protein in sympathetic and sensory neurons correlate with early postmortem studies of individuals with FD who showed dramatic reduction in the number of sensory, sympathetic and some parasympathetic neurons (Axelrod et al., 1981; Pearson and Pytel, 1978; Pearson et al., 1978). The physiological impairments caused by sensory and sympathetic neuron loss are present from birth and appear to progress with age, but how Elp1 functions and whether it is required in adult neurons remains unknown.

Elp1 has been implicated in actin and microtubule network remodeling necessary for neuron differentiation, migration and target tissue innervation (Cheishvili et al., 2011; Close et al., 2006; Johansen et al., 2008). Accordingly, reduction of Elp1 in embryonic mouse cortical neurons has been shown to delay their migration along radial glial cells to the cortical plate in addition to altering their dendritic morphology (Creppe et al., 2009). Given the importance of migration and differentiation of neural crest cells (NCCs), which give rise to sympathetic and sensory neurons during development, FD could be caused by impaired NCC migration and/or differentiation (Naumanen et al., 2008). However, many of the *in vitro* studies that have examined the functional consequences of Elp1 depletion have been performed in cellular contexts apart from that in which disease occurs, and *in vivo* studies to understand the function of Elp1 during mammalian sensory and sympathetic nervous system development have been hindered because loss of Elp1 in all tissues leads to embryonic lethality, which is not a common manifestation of the disease (Chen et al., 2009; Dietrich et al., 2011). Recent studies using shRNA to reduce Elp1 in chick NCCs (Hunnicutt et al., 2012) or to ablate it in mouse NCCs (George et al., 2013) indicate that Elp1 is not required for NCC migration, but how it functions in post-migratory neuron differentiation and/or target tissue innervation is still poorly understood.

To define the *in vivo* role of Elp1 during NCC migration, differentiation and sympathetic/sensory neuron target tissue innervation, we generated conditional *Elp1* KO (cKO) mice. Ablation of Elp1 in NCCs bypassed embryonic lethality that occurs in germline *Elp1* knockout mice, and in agreement with previous

Development (2014) 141, 2452-2461 doi:10.1242/dev.107797

results, it had no detectable role in their migration (George et al., 2013; Hunnicutt et al., 2012). In addition, we found that loss of Elp1 in NCCs did not alter sensory and sympathetic neuron proliferation or survival prior to their target tissue innervation, but at later stages of development profound abnormalities in neuron survival and target tissue innervation were identified. Ablation of Elp1 in fate-specified sympathetic neurons resulted in similar neuron survival and target tissue abnormalities, confirming that Elp1 has a sympathetic neuron autonomous role in target tissue innervation that is independent of its function in other cells derived from NCCs. Moreover, sympathetic target tissue innervation abnormalities were correlated with sympathetic neuron cytoskeletal organization and neurite outgrowth abnormalities *in vitro*. Thus, sympathetic and sensory neuron loss in individuals with FD is primarily caused by target tissue innervation failure during development and with age, rather than by major alterations in Elp1-dependent neuron survival, differentiation or migratory capacity. The microtubule alterations observed in Elp1-deficient neurons support the concept that it has a role in neuron microtubule dynamics that may be essential for normal axon extension and guidance during target tissue innervation and for innervation homeostasis.

RESULTS

Generating viable Elp1 conditional knockout mice

The underlying mechanism leading to differential vulnerability of peripheral sensory and sympathetic neurons in FD is thought to relate to relatively poor Elp1 splicing and inadequate levels of functional protein within them. *Elp1* is ubiquitously expressed and knockout mice lacking Elp1 in all cells die at mid-gestation (Chen et al., 2009; Dietrich et al., 2011), prior to peripheral neuron precursor migration, differentiation or target tissue innervation. In humans with FD, a germline point mutation in intron 20 leads to exon 20 skipping and to Elp1 loss in sympathetic and sensory neurons due to protein truncation ($Elp1_{Tr}$, Fig. 1A, top). To examine Elp1 function in FD disease-vulnerable cells, cell-specific exon 20 skipping was facilitated by introducing loxP sites into the mouse genome that flank exon 20 (Fig. 1A, bottom) and mating them to cell lineage-specific Cre-recombinase-expressing mice.

The Elp1-flx targeting construct (Fig. 1B) was electroporated into C57BL/6 embryonic stem (ES) cells and correctly targeted clones were identified using PCR and Southern blotting on genomic DNA isolated from them (Fig. 1C,D). Targeted clones that contained a correctly targeted Frt site-flanked Neo expression cassette were injected into C57BL/6 blastocysts to generate chimeric mice carrying the targeted Neo allele in the germline. Heterozygous ($Elp1^{+/Neo}$) progeny derived from mating with C57BL/6 mice were mated to CAG-Flpe mice to remove the Frt site-flanked Neo cassette from the germline, to generate the final exon 20 loxP site-flanked allele ($Elp1^{+/f}$). Heterozygous ($Elp1^{+/f}$) mice were identified by PCR using genomic DNA isolated from tail biopsy tissue (Fig. 1E) and they were intercrossed to generate homozygous ($Elp1^{f/f}$) mice.

Heterozygous intercrosses ($Elp1^{+/f}\times Elp1^{+/f}$) generated newborn mice with the expected Mendelian Elp1 allelic frequencies (n=106 pups; χ^2 test, P=0.52). Homozygous $Elp1^{f/f}$ mice did not show obvious gross abnormalities or dysmorphisms (supplementary material Fig. S1A), but by 3 weeks of age (P21) at the time of weaning, their weight was ~50% of that of wild-type ($Elp1^{+/+}$) littermates (supplementary material Fig. S1B). Homozygous $Elp1^{f/f}$ mice continued to weigh significantly less than wild-type littermates, at least during the first 6 weeks of life when postnatal weights were monitored ($F_{1,76}$=107.0, P<0.0001). Although close to 20% of both wild-type and $Elp1^{f/f}$ mice were lost within the first week of age due to natural attrition, there was an additional 20% of $Elp1^{f/f}$ mice lost after weaning at P21 (supplementary material Fig. S1C). The Elp1-flx allele was moderately hypomorphic as quantitative analysis using western blotting to detect Elp1 protein in brain, DRG and superior cervical

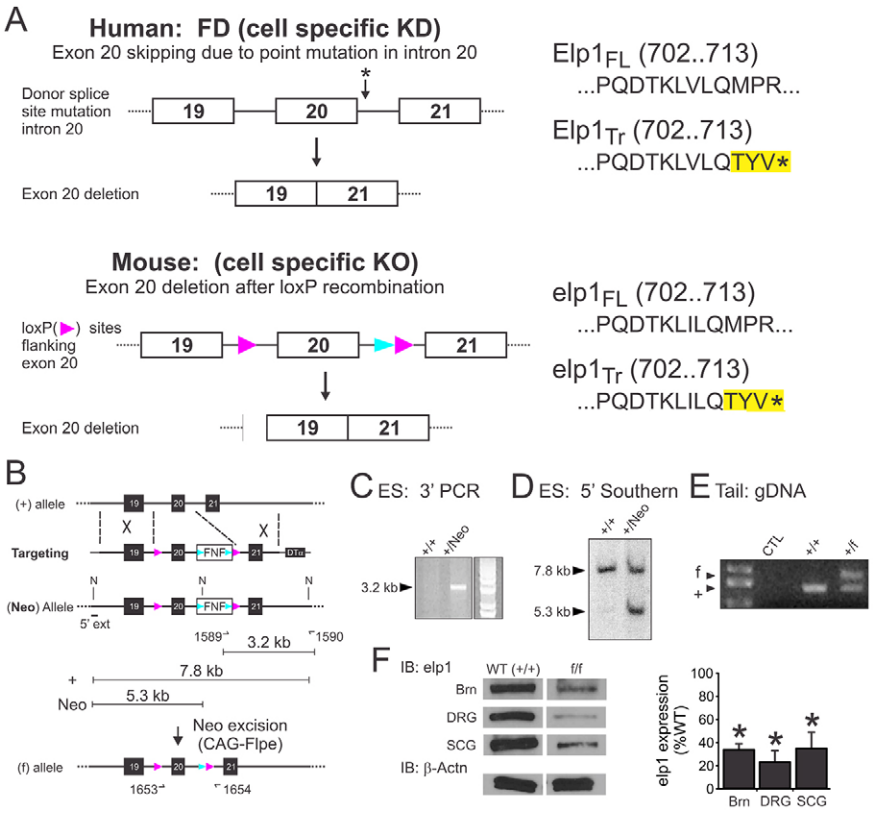

Fig. 1. Generating Elp1 conditional loss-of-function mice. (A, top) In humans, a germline T→C point mutation in the donor splice site of intron 20 (asterisk) leads to skipping of exon 20 during primary transcript splicing in FD. Loss of exon 20 in the spliced mRNA introduces a nonsense mutation that results in Elp1 protein truncation ($Elp1_{Tr}$) during translation. (A, bottom) The mouse *Elp1* gene was mutated by targeting loxP sites to intron 19 and 20. In Cre-recombinase-expressing cells, exon 20 is removed by recombination of flanking loxP sites, leading to Elp1 protein truncation ($Elp1_{Tr}$) similar to human FD. (B) A forward-oriented loxP site was introduced into intron 19 and a Frt-site-flanked Neo cassette into intron 20 (*N*=*Nhe*I restriction sites). (C) Long-range PCR using primers (OT1589 and OT1590) that span the 3′ recombination arm of the targeting construct showed the appropriate recombination event in appropriately targeted G418-selected ES cell DNA clones. (D) *Nhe*I-restricted genomic DNA isolated from PCR-positive ES cell clones was used to identify the 5′ homologous recombination event by Southern blotting. (E) Germline transmission of the Neo-deleted flx (*f*) allele was identified by PCR on genomic DNA template isolated from tail biopsy tissue. (F) $Elp1^{f/f}$ mice were viable, but tissues from $Elp1^{f/f}$ mice produced 30-40% of the level of Elp compared with tissues from $Elp1^{+/+}$ mice. Brn, brain; DRG, dorsal root ganglia; SCG, superior cervical ganglia. Results represent western blot densitometry measurements of wild-type normalized mean±s.e.m. from n=3 wild type ($Elp1^{+/+}$) and $Elp1^{f/f}$ tissues; *P<0.01, Student's t-test.

Development (2014) 141, 2452-2461 doi:10.1242/dev.107797

ganglia (SCG) showed significantly reduced Elp1 protein relative to the wild-type allele (Fig. 1F, $P<0.01$, Student's *t*-test). Germline heterozygous (*Elp1*$^{+/-}$) mice, which have a 50% reduction of Elp1 protein in all tissues, are normal (Chen et al., 2009; Dietrich et al., 2011) and these results indicate that even reduction of Elp1 protein to 30-40% of the normal level is sufficient for survival. As *Elp1*$^{f/f}$ mice aged, they developed progressive neurological abnormalities, including ptosis and altered gait (data not shown), suggesting that reduced levels of Elp1 in these mice could emulate phenotypes observed in humans with FD. Functional ablation of Elp1 in *Elp1*$^{f/f}$ mice was confirmed using SCG sympathetic neurons isolated from *Elp1*$^{+/+}$ and *Elp1*$^{f/f}$ mice. Neurons infected with a Cre-recombinase-expressing adenovirus (AdCre) showed the expected deletion of exon 20 from the Elp1 transcript (Δ20) and the resulting nonsense mutation (Fig. 2A), similar to that which occurs in human disease (Fig. 1A).

Elp1 ablation in Wnt1-expressing neural crest-derived cells results in abnormal palatogenesis

Sensory and sympathetic neurons are lost in FD, and previous data have suggested that cellular migration and/or differentiation may be impaired in the absence of Elp1 (Creppe et al., 2009; Naumanen et al., 2008). Therefore, we reasoned that sensory and sympathetic neurons may be lost in FD if they do not migrate or differentiate properly during development. *Elp1*$^{+/f}$ mice were mated to Wnt1-Cre transgenic mice that express Cre-recombinase in Wnt1-specified pre-migratory and migratory NCCs, from which sympathetic and sensory neurons derive (Raible and Ungos, 2006; Rohrer, 2011). In some experiments R26R Cre-recombinase reporter mice were used to trace the fate of Wnt1-specified cells *in vivo* (Soriano, 1999). Genomic DNA isolated from newborn DRG and SCG neurons showed efficient recombination of the Elp1-flx allele to generate the

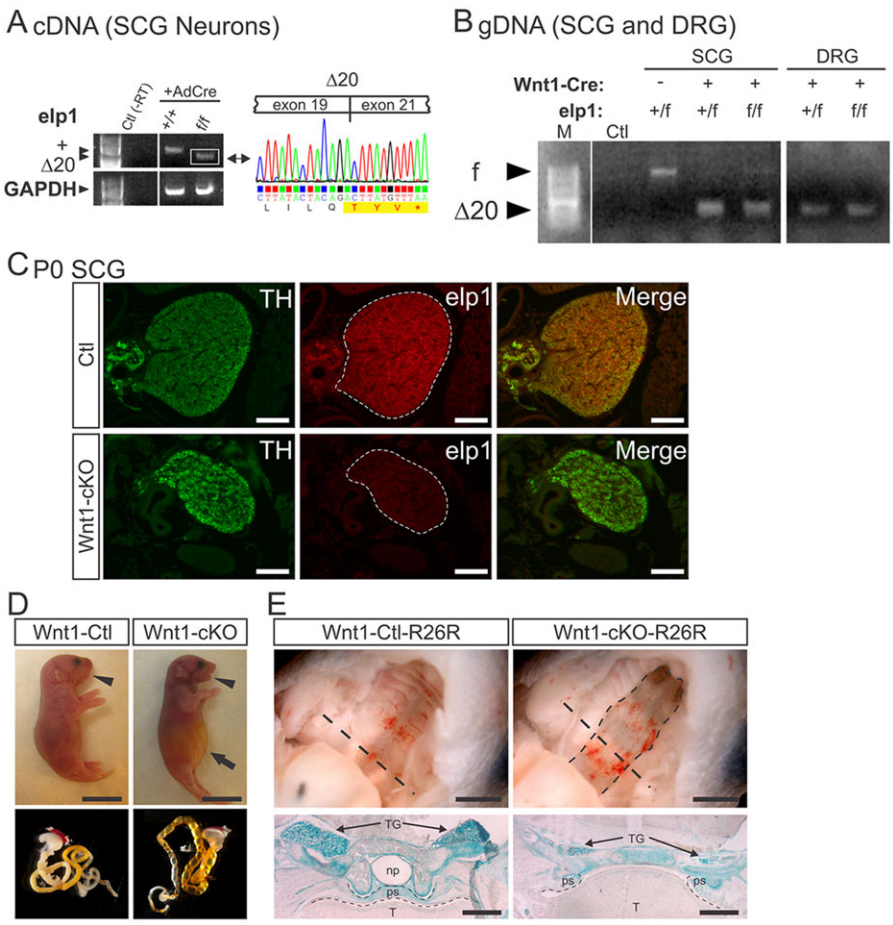

Fig. 2. Conditional ablation of Elp1 in neural crest-derived cells (NCCs) results in death at birth and abnormal palatogenesis. (A) Sequence analysis of PCR amplified Elp1 cDNA of exon 19-21 from *Elp1*$^{+/+}$ and *Elp1*$^{f/f}$ sympathetic neurons infected with Adeno-Cre virus showed efficient exon 20 deletion (Δ20) and the predicted nonsense mutation leading to Elp1 truncation. GAPDH amplification was used as positive control and no reverse transcriptase (Ctl) as negative control for cDNA PCR amplification. (B) Wnt1-Cre transgenic mice produced efficient exon 20 deletion (Δ20) *in vivo* in *Elp1*$^{+/f}$ and *Elp1*$^{f/f}$ SCG and DRG neurons. Genomic DNA (gDNA) from newborn SCG and DRG was amplified by PCR with oligonucleotides that amplified the flx (f) allele and the exon 20-excised (Δ20) allele. Ctl, no genomic DNA template. (C) Tyrosine hydroxylase (TH, green) and Elp1 (red) immunofluorescence showed complete ablation of Elp1 in newborn *Wnt1-Cre*$^{+}$*;Elp1*$^{f/f}$ (Wnt1-cKO) SCG. Scale bars: 100 μm. (D, top) Newborn Wnt1-cKO mice were born alive but died shortly after birth and they had mild facial dysmorphisms characterized by a slightly recessed mandible (retrognathia, arrowhead) compared with *Wnt1-Cre*$^{+}$*;Elp1*$^{+/+}$ (Wnt1-Ctl) mice. In addition, Wnt1-cKO mice exhibited a gasping behavior immediately following birth and they had a distended abdomen (arrow) with (bottom) an air-filled gastrointestinal tract. Scale bars: 0.5 cm. (E, top) Ventral view of the soft and hard palate (roof of the mouth after the mandible was cut away for visual access) showed a cleft palate in Wnt1-cKO mice (dashed outline). (E, bottom) In mice that also carried the R26R Cre-recombinase reporter allele, *lacZ* histochemistry on coronal sections through the head, at the level indicated by the straight dashed lines (top), identified the cells derived from the Wnt1-expressing neural crest stained in blue. In *Wnt1-Cre*$^{+}$*;Elp1*$^{+/+}$*;R26R*$^{+/f}$ (Wnt1-Ctl-R26R) mice the intact palatal shelf (ps) separated the oral cavity occupied by the tongue (T) from the nasopharynx (np). *Wnt1-Cre*$^{+}$*;Elp1*$^{f/f}$*;R26R*$^{+/f}$ (Wnt1-cKO-R26R) mice had a 100% penetrant cleft palate caused by failure of the palatal shelf (ps) and soft palate to fuse, resulting in the tongue protruding into the nasopharynx to occlude the airway. TG, trigeminal ganglia; ps, palatal shelf. Scale bars: 2 mm (top); 500 μm (bottom).

Development (2014) 141, 2452-2461 doi:10.1242/dev.107797

Δ20 allele (Fig. 2B), which was accompanied by loss of detectable Elp1 protein as expected (Fig. 2C, newborn SCG shown).

Wnt1-Cre^{+}*;Elp1*$^{f/f}$ (Wnt1-cKO) mice were born at the expected Mendelian frequency (n=129 pups; χ^2 test, P=0.58), but all of them died within a few hours of birth, accounting for abnormalities in the expected ratios of surviving pups 14-21 days after birth (n=81 pups, χ^2 test, P<0.02). Wnt1-cKO mice showed no body dysmorphisms, but could be readily distinguished from littermates by a slightly recessed mandible (retrognathia; Fig. 2D, arrowhead), similar to humans with FD (Mass et al., 1998), their labored breathing (supplementary material Movie 1) and their distended abdomen (Fig. 2D, arrow). An air-filled stomach and loops of bowel that contained no milk in most mutant pups appeared to be the cause of the protuberant abdomen (Fig. 2D, bottom). Macroscopic examination of the oral cavity in Wnt1-cKO mice revealed complete clefting of the secondary palate that was 100% penetrant (Fig. 2E, top). Coronal sections through the nasopharynx (np), palate and oropharynx of newborn Wnt1-cKO mice demonstrated a failure in soft palate and palatal shelf (ps) fusion, resulting in protrusion of the tongue (T) into the nasopharynx (np), presumably leading to asphyxiation (Fig. 2E, bottom).

As Wnt1-specified NCCs are known to give rise to craniofacial mesenchyme that produce many facial bones such as the mandible, frontal and nasal bones (Cordero et al., 2011), we used Alizarin Red and Alcian Blue stains to analyze cranial bone formation in newborn Wnt1-cKO mice. Although the bone development that makes up the palatine skeleton was completely absent (supplementary material Fig. S2A, arrows), the skull bones were generally normally formed, but showed mild hypoplasia (supplementary material Fig. S2B), consistent with an overall preservation of craniofacial mesenchymal differentiation and migration in the absence of Elp1.

Normal migration, proliferation and survival of sensory and sympathetic neuron precursors in NCCs lacking Elp1

During development, NCCs undergo an epithelial-to-mesenchymal transition in the neural crest (NC) that leads to their migration from the dorsal neural tube along stereotypic routes to reach appropriate peripheral locations where they undergo lineage specification and differentiation (Fig. 3A). Previous studies indicate that Elp1 has a role in neuron migration (Close et al., 2006; Creppe et al., 2009; Lee et al., 2009). Thus, to examine whether Elp1 has a role in migration of NCCs fated to become sensory and sympathetic neurons, we isolated embryos from timed pregnant females at E12.5, a developmental time point when most migration had terminated and sensory and sympathetic neuron differentiation was under way (Murphy et al., 1993; Serbedzija et al., 1990). In E12.5 *Wnt1-Cre*$^{+}$*;Elp1*$^{+/+}$ (Wnt1-Ctl) embryos, *Elp1* was expressed at high levels in sensory and sympathetic neuroblasts, and it was ablated in Wnt1-cKO embryos, as expected (supplementary material Fig. S3A). However, there was no significant difference in the location and number of DRG and SCG neuroblasts between Wnt1-Ctl and Wnt1-cKO embryos (Fig. 3B,C). Similarly, immunohistochemistry using Ki67 or cleaved caspase 3 (CC3) showed no significant differences in the number of proliferating or apoptotic neuroblasts, respectively, between Wnt1-Ctl and Wnt1-cKO mutant embryos (Fig. 3B,C). That sensory, sympathetic and enteric neuron migration was not impaired in Wnt1-cKO mutants was additionally confirmed in newborn mice that carried the Rosa-26 (R26R) Cre-recombinase reporter to label Wnt1-specified cells (supplementary material Fig. S3B). The R26R reporter allows visualization of Wnt1-specified sympathetic chain ganglia, DRG, adrenal chromaffin cells and enteric neurons in whole-mount preparations and in tissue sections in *Wnt1-Cre*$^{+}$*;Elp1*$^{+/+}$*;R26R*$^{+/f}$ (Wnt1-Ctl-R26R) and *Wnt1-Cre*$^{+}$*;Elp1*$^{f/f}$*;R26R*$^{+/f}$ (Wnt1-cKO-R26R) (supplementary material Fig. S4). Although sympathetic ganglia such as the SCG and the sensory DRG were smaller in newborn Wnt1-cKO compared with Wnt1-Ctl mice (SCG=58.5±9.7% and DRG=62.2±9.1%; n=5 or 6 ganglia, P<0.05, Student's t-test), the neurons appeared to have migrated to their appropriate locations, as did adrenal chromaffin cells and enteric neurons [supplementary material Fig. S4A (bottom) and S4B].

Elp1 ablation in NCCs disrupts target tissue innervation, but not sympathetic and sensory neuron lineage specification

In FD, a marked reduction in sympathetic/sensory ganglion volume and neuron number is correlated with sensory and autonomic dysfunction (Axelrod, 2004; Axelrod et al., 1981), but it is not known whether neuron loss is due to impaired neuron fate specification, failed target tissue innervation or an intrinsic dependency on Elp1 function for neuron survival. We found that in the absence of Elp1, lineage-restricted molecules were appropriately expressed in newborn (post-migratory) sympathetic and sensory neurons. For example, although the SCG was smaller, sympathetic lineage-associated

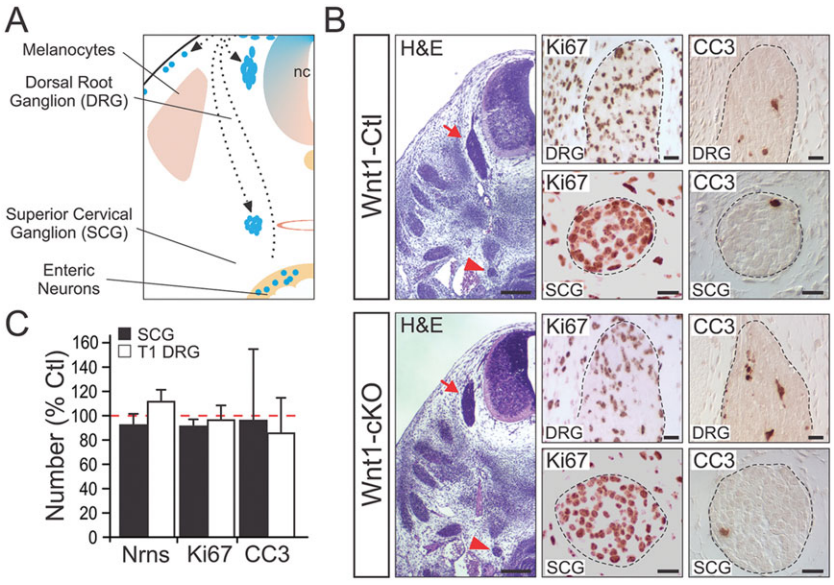

Fig. 3. Loss of Elp1 in Wnt1-expressing neural crest cells does not alter the survival or migration of neural crest-derived SCG or DRG neurons. (A) Many cell types, including sensory DRG and sympathetic neurons arise from neural crest cell (NCC) progenitors, and they migrate to their stereotypic locations prior to innervating target tissues. (B) By E12.5 in the mouse, DRG (red arrow) and SCG (red arrowhead) neurons have largely finished their migration to their characteristic locations. SCG and DRG neurons in Wnt1-Cre^{+}; Elp1$^{f/f}$ (Wnt1-cKO) mice migrate to their appropriate locations compared with *Wnt1-Cre*$^{+}$*;Elp1*$^{+/+}$ (Wnt1-Ctl) mice. (C) Immunohistochemistry for Ki67 and CC3 labels proliferating and apoptotic cells, respectively, and there were no differences in the number, proliferation or apoptosis of cells in the DRG and SCG between Wnt1-Ctl and Wnt1-cKO mice (results show mean±s.e.m. from three animals of each genotype and normalized to Wnt1-Ctl). Scale bars: 200 μm for H&E; 20 μm for Ki67 and CC3.

Development (2014) 141, 2452-2461 doi:10.1242/dev.107797

molecules such as tyrosine hydroxylase (TH), tropomyosin-related kinase A (TrkA), SCG10 and neuropeptide Y (NPY) were expressed in remaining Wnt1-cKO sympathetic neurons (supplementary material Fig. S5A). Similarly in the DRG, sensory modality-associated neurotrophic factor receptors TrkA (nociception), TrkB (cutaneous mechanosensation) and TrkC (proprioception) were also expressed in a subset of remaining Elp1-deficient sensory neurons similar to Wnt1-Ctl ganglia. However, although Wnt1-cKO DRG were small compared with Wnt1-Ctl ganglia, and TrkA+ and TrkB+ neurons were significantly diminished in number, TrkC+ neurons were not changed in number (supplementary material Fig. S5B). Taken together, the results indicate that sympathetic and sensory neurons derived from Elp1-deficient NCCs can express markers characteristic of their normal lineage specification.

To examine whether Elp1 has a role in innervation, representative target tissues that receive sensory and sympathetic innervation were compared between newborn Wnt1-Ctl and Wnt1-cKO mice. The glabrous footpad, which receives dense cutaneous nociceptive and mechanoceptive sensory innervation, was examined using peripherin (Prph) and heavy chain neurofilament (NF-H) immunohistochemistry (Honma et al., 2010). Cutaneous sensory innervation of footpads was profoundly abnormal in Wnt1-cKO mice where Prph+ and NF-H+ axon innervation was reduced to 6.8% and 11.0%, respectively (n=2 or 3 mice and >40 tissue sections analyzed per genotype, P<0.0001, Student's t-test) (Fig. 4). In addition, parvalbumin (Pv) immunohistochemistry was used as a well-established marker of proprioceptive sensory innervation to skeletal muscle stretch receptors (Albert et al., 2005; Tourtellotte et al., 2001), which was highly significantly reduced to 4.8% in Wnt1-cKO skeletal muscle compared with Wnt1-Ctl mice (n=2 mice and over 30 tissue sections analyzed per genotype, P<0.0001, Student's t-test) (Fig. 4). In the sympathetic nervous system, many target organs, including bowel, salivary gland, spleen, heart, kidney and stomach, were examined using whole-mount and tissue section TH immunohistochemistry. In all organs examined, TH+ sympathetic innervation visceral axon bundle branching was markedly diminished. For example, sympathetic innervation to the renin-expressing juxtaglomerular apparatus in the kidney was significantly decreased to 20.1% and axon bundle branching was

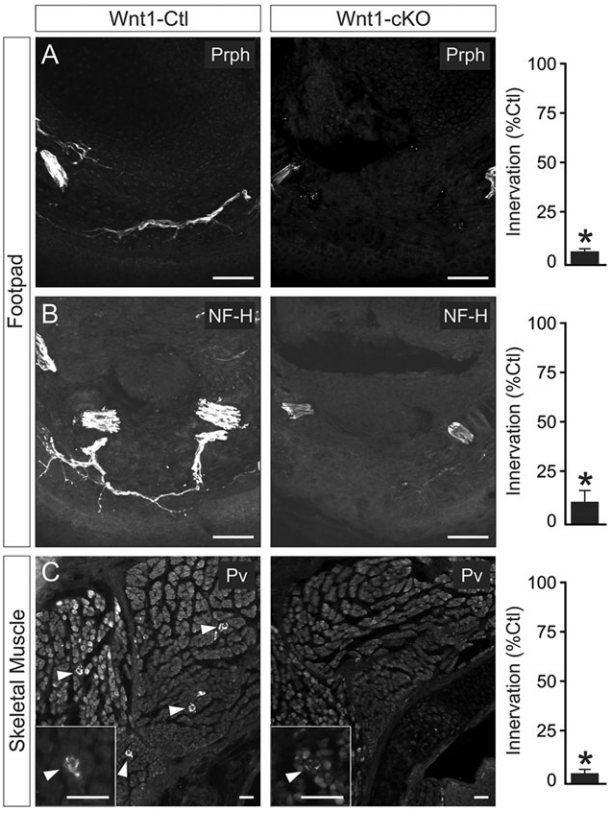

Fig. 4. Sensory neurons mediating differing sensory modalities poorly innervate target tissues in Wnt1-Cre^{+};Elp1$^{f/f}$ (Wnt1-cKO) mice. (A-C) Cutaneous innervation to the footpad identified by immunohistochemistry for peripherin (Prph), which primarily labels axons mediating pain and temperature sensation, and neurofilament-H (NF-H), which primarily labels axons mediating mechanosensation, were decreased by over 90% in Wnt1-cKO mice compared with *Wnt1-Cre*$^{+}$;*Elp1*$^{+/+}$ (Wnt1-Ctl) mice (Wnt1-Ctl normalized mean±s.e.m. total fluorescence intensity per unit area). In skeletal muscle, parvalbumin (Pv) labeled proprioceptive sensory innervation to muscle spindle stretch receptors was decreased by over 90% in Wnt1-cKO relative to Wnt1-Ctl mice (Wnt1-Ctl normalized mean±s.e.m. of Pv+ innervated stretch receptor profiles per section). Results are from three animals of each genotype; *P<0.001, Student's paired t-test. Scale bars: 70 μm.

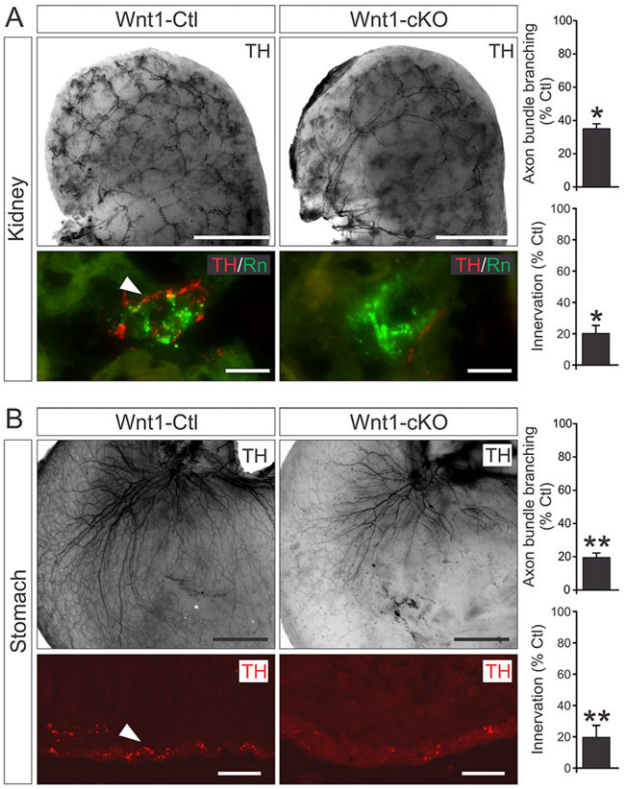

Fig. 5. Sympathetic target tissue innervation is impaired in *Wnt1-Cre*$^{+}$;*Elp1*$^{f/f}$ (Wnt1-cKO) mice. Whole-mount and tissue section tyrosine hydroxylase (TH) immunohistochemistry showed target tissue innervation and visceral axon bundle branching abnormalities in newborn Wnt1-cKO compared with *Wnt1-Cre*$^{+}$;*Elp1*$^{+/+}$ (Wnt1-Ctl) mice. (A) Abnormal renal innervation was characterized by (top) decreased innervation that primarily terminated in the (bottom) renin (Rn)-expressing juxtaglomerular body. Visceral axon bundle branching was reduced by over 60% and innervation by over 80% in Wnt1-cKO mice. Scale bars: 0.5 mm (top); 25 μm (bottom). (B, top) Whole-mount TH immunohistochemistry of the stomach also showed decreased sympathetic axon bundle branching in newborn Wnt1-cKO mice that correlated with (bottom) decreased innervation to the smooth muscle wall using TH immunohistochemistry in tissue sections. Scale bars: 0.5 mm (top); 25 μm (bottom). Innervation was determined as total fluorescence intensity per unit area; mean±s.e.m. innervation and axon bundle branching from three animals of each genotype and normalized to Wnt1-Ctl; *P<0.001 and **P<0.01, Student's paired t-test.

Development (2014) 141, 2452-2461 doi:10.1242/dev.107797

decreased to 34.9% (n=2 mice and over 30 tissue sections of each genotype analyzed, P<0.05 and P<0.0001, respectively, Student's t-test) compared with Wnt1-Ctl animals (Fig. 5A). Similarly, sympathetic innervation to the gastric smooth muscle was also diminished to 19.7% and axon bundle branching was decreased to 19.6% (n=2 mice and over 30 tissue sections of each genotype analyzed, P<0.0001, Student's t-test) compared with Wnt1-Ctl animals (Fig. 5B). Although neuron loss very likely contributed to the overall decreased sympathetic and sensory target tissue innervation, remaining visceral axon bundles ramified poorly within target tissues in the absence of Elp1.

Sensory and sympathetic target tissue innervation abnormalities were associated with neuron loss as a consequence of apoptosis (Fig. 6A, newborn DRG shown). To determine whether Elp1 has a neuron autonomous role in survival, *Elp1*$^{+/+}$ (Ctl) and *Elp1*$^{f/f}$ SCG and DRG neurons were isolated from newborn mice and infected with adenovirus that expresses both Cre-recombinase and eGFP (Ad-Cre-eGFP) to efficiently ablate Elp1 in *Elp1*$^{f/f}$-infected neurons (KO; Fig. 2A). Sensory and sympathetic neurons require NGF for survival and accordingly a highly significant dose-response effect of NGF concentration on neuron survival for Ctl and KO neurons was observed as expected (SCG: $F_{2,8}$=27; P<0.003; DRG: $F_{2,7}$=73; P<0.001). However, no significant effect of genotype on neuron survival was observed for differing concentrations of NGF (SCG: $F_{1,8}$=1.23; P=0.34; DRG: $F_{1,7}$=1.2; P=0.30) (Fig. 6B). Thus, Elp1 is not essential for sensory and sympathetic neuron survival, suggesting that *in vivo* neuron death is most likely a secondary consequence of failure of Elp1-deficient neurons to properly innervate their targets and acquire appropriate survival factor signaling.

Elp1 has a cell-autonomous role in target tissue innervation by lineage-specified sympathetic neurons

Wnt1 signaling has a relatively broad role in specifying neuronal, glial and mesenchymal cell fate during early embryogenesis (Sylvie et al., 2011), so it is not clear whether ablation of Elp1 in migratory precursor NCCs reflects a cell-autonomous function of Elp1 in fate-specified sympathetic and sensory neurons. To determine whether Elp1 has a role in neurons after they have been fate specified, we focused on sympathetic neurons and used dopamine β-hydroxylase (DβH)-iCre transgenic mice to selectively ablate Elp1 in lineage-specified sympathoblasts (Parlato et al., 2007). In some experiments we also used *StLa*$^{+/f}$ mice, which express axon localized *lacZ* (τlacZ) in Cre-recombinase-expressing cells (Nam and Benezra, 2009). In *DβH-iCre*$^{+}$;*Elp1*$^{+/+}$;*StLa*$^{+/f}$ (DβH-Ctl-StLa) mice, it was possible to visualize the sympathetic chain ganglia and their proximal axon processes (supplementary material Fig. S6A,B). Similar to the results obtained using Wnt1-Cre driver mice, the SCG (supplementary material Fig. S6A) and thoracic chain ganglia (supplementary material Fig. S6B) were markedly smaller in *DβH-iCre*$^{+}$;*Elp1*$^{f/f}$;*StLa*$^{+/f}$ (DβH-cKO-StLa) mice and many proximal axon processes were missing or highly attenuated compared with DβH-Ctl-StLa mice (supplementary material Fig. S6A,B). Whole-mount TH immunohistochemistry in newborn mice revealed clear target tissue innervation abnormalities in DβH-cKO mice (Fig. 7). Although overall innervation was diminished and correlated with marked sympathetic neuron apoptosis (data not shown), the remaining visceral axon bundles also appeared to have markedly attenuated branching in all tissues examined. For example, axon bundle branching in salivary gland, kidney, heart and spleen was reduced to 33%, 15%, 16% and 29%, respectively, compared with DβH-Ctl mice.

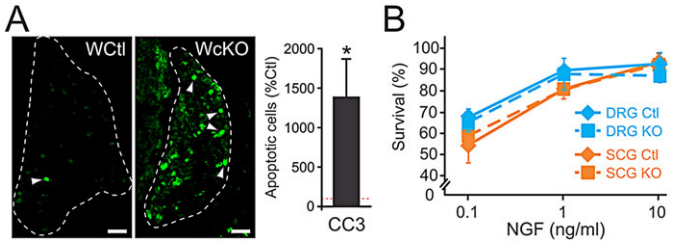

Fig. 6. Elp1 is not directly required for sympathetic and sensory neuron survival, despite increased neuron death in *Wnt1-Cre*$^{+}$;*Elp1*$^{f/f}$ (WcKO) mice. (A) There was nearly a 15-fold increase in apoptotic neuron death in Wnt1-cKO DRG (and SCG, not shown) compared with *Wnt1-Cre*$^{+}$;*Elp1*$^{+/+}$ (WCtl), as measured by cleaved caspase 3 (CC3) immunohistochemistry. Scale bars: 50 μm. Data are mean±s.e.m. of CC3-labeled apoptotic cells from three animals of each genotype and are normalized to WCtl; *P<0.001, Student's t-test). Arrowheads indicate representative CC3+ (apoptotic) cells. (B) SCG sympathetic and DRG sensory neurons isolated from *Elp1*$^{+/+}$ and *Elp1*$^{f/f}$ mice were infected with Ad-Cre-eGFP virus and differentiated in the presence of 0.1, 1.0 and 10 ng/ml of NGF. The fraction of infected *Elp1*$^{+/+}$ (Ctl) and *Elp1*$^{f/f}$ (KO) neurons surviving was quantified by counting the number that were not labeled by CC3 relative to the total number of infected neurons. Neither sympathetic ($F_{1,8}$=1.23; P=0.34) nor sensory ($F_{1,7}$=1.2; P=0.61) neurons showed any significant difference in survival between wild-type (Ctl) and Elp1-deficient (KO) neurons (mean±s.e.m. of three independent experiments).

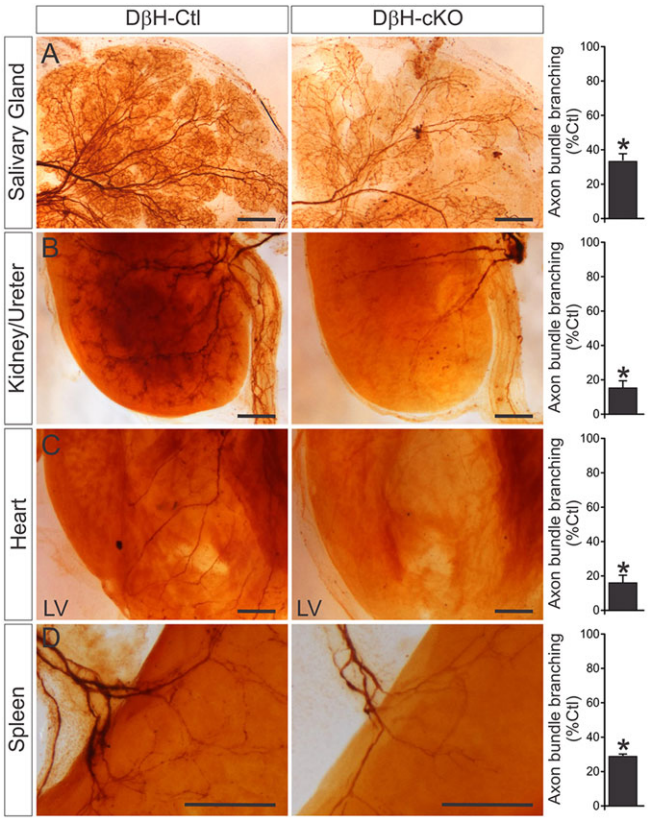

Fig. 7. Elp1 has a sympathetic neuron autonomous role in target tissue innervation. (A-D) Ablation of Elp1 in lineage-specified sympathetic neurons in *DβH-iCre*$^{+}$;*elp*$^{f/f}$ (DβH-cKO) mice showed highly diminished sympathetic target tissue innervation and visceral axon bundle branching using whole-mount TH staining in (A) salivary gland, (B) kidney/ureter, (C) heart and (D) spleen compared with *DβH-iCre*$^{+}$;*Elp1*$^{+/+}$(DβH-Ctl) mice. Axon bundle branching within the analyzed target organs was reduced by 70-80%. Scale bars: 250 μm. Data are mean±s.e.m. from three animals of each genotype and are normalized to results from DβH-Ctl mice; *P<0.002, Student's t-test).

Development (2014) 141, 2452-2461 doi:10.1242/dev.107797

Impaired neurite outgrowth and branching in Elp1-depleted sympathetic and sensory neurons is associated with abnormal cellular microtubule aggregation

Analysis of DβH-cKO mice indicates that Elp1 has a sympathetic neuron autonomous function in target tissue innervation. To examine Elp1 function in neurite outgrowth and branching, sympathetic neurons from *Elp1*$^{f/f}$ mice were isolated and infected with Ad-Cre-eGFP virus (Fig. 2). Complete loss of Elp1 in sympathetic neurons resulted in a significant decrease in total neurite length and branching compared with *Elp1*$^{+/+}$ infected neurons (Fig. 8A). Similar results were obtained using shRNA molecules that were previously characterized to deplete Elp1 (Creppe et al., 2009) and reconfirmed in neuroblastoma N2a cells (supplementary material Fig. S7). Reduction of Elp1 resulted in a significant decrease in total neurite outgrowth and branching in sympathetic (supplementary material Fig. S8A) and sensory (supplementary material Fig. S8B) neurons, and the effects were rescued in sympathetic neurons by co-transfecting human Elp1 (help1) not subject to shRNA-mediated degradation (supplementary material Fig. S8A).

Previous studies indicate that Elp1 depletion results in loss of lysine acetyltransferase activity mediated by its binding partner Elp3. Indeed, α-tubulin acetylation (Ac-αTub) was reported to be decreased in neurons after shRNA-mediated knockdown of Elp1 and to alter their morphology and migration during development (Creppe et al., 2009; Solinger et al., 2010). To examine whether Ac-αTub was altered in the absence of Elp1, immunohistochemistry was used on *Elp1*$^{+/+}$ (WT) and *Elp1*$^{f/f}$ (KO) sympathetic neurons infected with Ad-Cre-eGFP virus and on tissue sections containing the SCG from newborn Wnt1-Ctl and Wnt1-cKO mice. No significant difference in Ac-αTub fluorescence intensity was found between WT and KO neurons *in vitro* (Fig. 8B) or in Elp1-deficient SCG neurons *in vivo* (Fig. 8C).

Recent studies have also indicated that Elp1 may regulate microtubule (MT) dynamics since tyrosinated α tubulin (Y-αTub), a marker of the unstable pool of tubulin within cells, was found to be abnormally distributed in human FD fibroblasts and in cells with depleted Elp1 using shRNA-mediated interference (Cheishvili et al., 2011). As MTs represent an essential component of the dendritic and axonal cytoskeleton of neurons, we examined Y-αTub distribution in *Elp1*$^{+/+}$ and *Elp1*$^{f/f}$ sympathetic neurons that were infected with Ad-Cre-eGFP virus (Ctl and KO neurons, respectively) using immunohistochemistry. Consistent with previous results (Cheishvili et al., 2011), Elp1 KO neurons showed a significantly disorganized pattern of Y-αTub distribution with prominent perinuclear accumulation (Fig. 8D). Relative destabilization of MTs in Elp1-deficient neurons may account for their abnormal neurite outgrowth and branching, but how Elp1 influences microtubule stability remains unclear. For example, recent studies proposed that loss of Elp1 leads to a loss of RE-1-silencing transcription factor (Rest), which in turn leads to an increase in stathmin 2 expression (Stmn2/Scg10), which is normally repressed by Rest. As Stmn2 has a major role in neuron MT destabilization (Mori and Morii, 2002), decreased Rest and consequent increased Stmn2 expression was proposed to account for increased levels of soluble Y-αTub and disorganized MTs in cells with low Elp1 levels. Surprisingly, however, in differentiating *Elp1*$^{+/+}$ and Elp1 KO sympathetic and sensory neurons, we found a significant

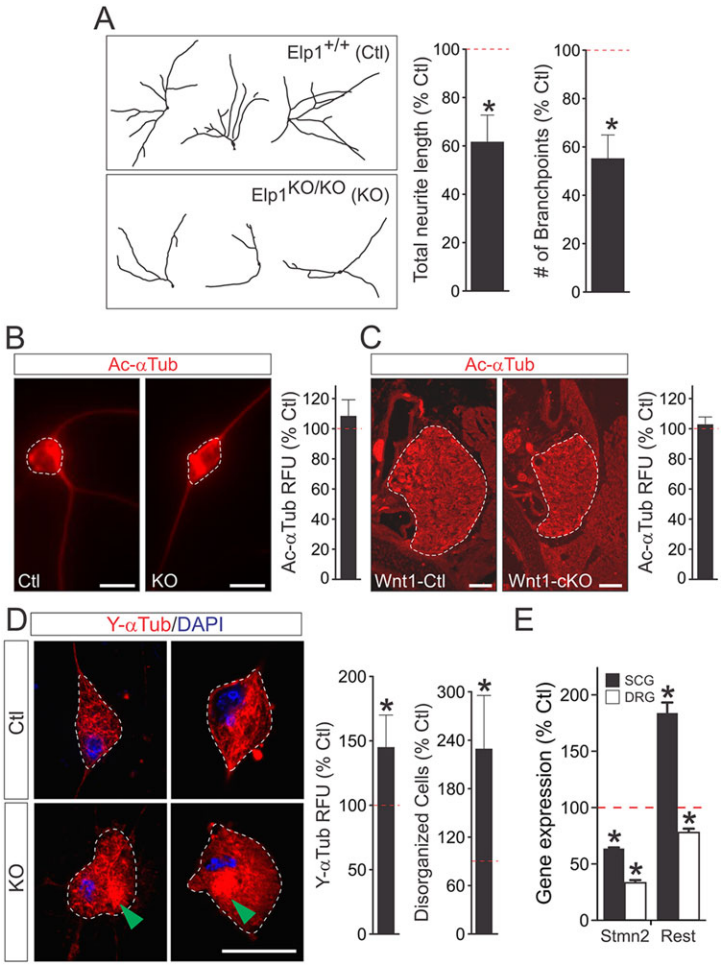

Fig. 8. Elp1-deficient neurons have neurite outgrowth and branching abnormalities that are associated with altered intracellular tyrosinated α-Tubulin (Y-αTub) localization. (A) Neurite outgrowth and branching was significantly attenuated in Ad-Cre-eGFP virus infected *Elp1*$^{f/f}$ (KO) sympathetic neurons compared with virus-infected *Elp1*$^{+/+}$ (Ctl) sympathetic neurons (data are percentage mean± s.e.m. of KO compared with Ctl values from triplicate experiments with over 30 neurons quantified for each condition; **P*<0.01, Student's *t*-test). (B) Acetylated α-tubulin (Ac-αTub) was not found to be decreased in differentiated AdCre-eGFP-infected *Elp1*$^{f/f}$(KO) sympathetic neurons compared with infected *Elp1*$^{+/+}$ (Ctl) sympathetic neurons. Scale bars: 20 μm. Data are percentage mean±s.e.m. of fluorescence intensity per neuron cell body area for KO neurons normalized to the fluorescent intensity per cell body area in Ctl neurons and repeated in triplicate separate experiments; *P*=0.15, Student's *t*-test. (C) Similarly, no difference in Ac-αTub was observed in tissue sections of SCG lacking Elp1 from newborn *Wnt1-Cre*$^{+}$*;Elp1*$^{f/f}$ (Wnt1-cKO) mice. Scale bars: 100 μm. Data are the percentage mean±s.e.m. of fluorescence intensity per cross-sectional area of SCG in Wnt1-cKO mice normalized to values from Wnt1-Cre^{+};Elp1$^{+/+}$ (Wnt1-Ctl) mice from *n*=2 animals of each genotype and representing over 15 tissue sections analyzed per genotype; *P*=0.76, Student's *t*-test). (D) Levels of tyrosinated α-tubulin (Y-αTub), a marker of destabilized microtubules, were significantly increased in KO sympathetic neuron somata compared with Ctl neurons and there were two or three times as many KO neurons that showed visibly recognizable perinuclear Y-αTub accumulation (arrowheads) compared with Ctl neurons. Scale bar: 20 μm. Data are percentage mean±s.e.m. of fluorescence intensity per soma cross-sectional area of KO neurons normalized to Ctl neurons from over 50 neurons analyzed per condition; *P*<0.01, Student's *t*-test. (E) In differentiated sympathetic SCG and sensory DRG neurons that lacked Elp1, Stmn2 was significantly downregulated, whereas Rest was significantly upregulated in sympathetic neurons and slightly downregulated in DRG neurons. Data are the percentage mean±s.e.m. of gene expression determined by qPCR performed in triplicate from three animals of each genotype and normalized to values obtained from Ctl neurons; **P*<0.01, Student's *t*-test.

Development (2014) 141, 2452-2461 doi:10.1242/dev.107797

decrease in Stmn2 in both SCG sympathetic and DRG sensory neurons, and an increase in Rest expression in sympathetic SCG neurons and a slight decrease in DRG sensory neurons. Although changes in the expression of Stmn2 and Rest are present in sympathetic and sensory neurons in the absence of Elp1, the changes in gene expression are essentially opposite from those previously reported (Cheishvili et al., 2011). Thus, the mechanism by which Elp1 influences microtubule dynamics within neurons and whether it has a physiologically significant role in the pathogenesis of FD requires additional investigation.

DISCUSSION

Elp1 is a component of the highly conserved hexameric (Elp1-6) transcriptional elongator complex (Otero et al., 1999). Several studies have examined transcriptional deregulation in cells isolated from individuals with FD or in heterologous cells after reduction of Elp1 by shRNA-mediated interference, but how the myriad of genes identified as potential Elp1 targets have a role in sympathetic and sensory neuron target tissue innervation in FD remains unclear (Cheishvili et al., 2007; Close et al., 2006; Cohen-Kupiec et al., 2011; Lee et al., 2009). Several studies have implicated Elp1 in cell migration, such as through its interaction with filamin A to regulate actin cytoskeleton reorganization during migration (Johansen et al., 2008) or by regulating α-tubulin acetylation in stabilized MTs, which are essential for neuron migration, neurite outgrowth and intracellular trafficking (Creppe et al., 2009; Solinger et al., 2010). However, previous studies in chick using shRNA to knockdown Elp1 in migrating NCCs (Hunnicutt et al., 2012) and more recent studies in mice that ablate Elp1 in migrating NCCs found no abnormalities in their migration (George et al., 2013). In agreement with these results, we found no changes in DRG or SCG location, neuron number, apoptosis or proliferation in the absence of Elp1 in E12.5 embryos after most NCC migration was complete. However, Elp1 appeared to have a role in some NCC-derived craniofacial mesenchymal cells as retrognathia, mild hypoplasia of the cranial bones and cleft palate were observed in newborn Wnt1-cKO mice. Whether this reflects mesenchymal cell migration, specification or differentiation abnormalities was not specifically studied, but it is interesting to note that mice lacking filamin A, which interacts with Elp1 in mesenchymal cells (Johansen et al., 2008), have a cleft palate similar to Wnt1-cKO mice (Hart et al., 2006). Additional studies will be required to better understand whether Elp1 has any role in regulating filamin A function in Wnt1-specified mesenchymal cells during craniofacial bone and palate development.

Although it seems possible that the developmental time points analyzed were not identical, our results differ from those obtained by George et al. (George et al., 2013) who attributed Elp1-dependent sensory neuron loss at E12.5 to increased apoptosis caused by premature neuroblast cell cycle exit and differentiation. Although we could not confirm sensory or sympathetic neuron loss at E12.5, our results indicated that most neuron loss is likely due to target tissue innervation abnormalities in the absence of Elp1, rather than to relatively minor abnormalities in neurogenesis or differentiation. For example, long after neuron specification would have occurred in newborn wild-type mice we observed increased neuron death in newborn Wnt1-cKO mice and we found that non-apoptotic neurons expressed appropriate lineage-associated markers in DRG and sympathetic ganglia. Interestingly, Elp1-deficient TrkC+ (proprioceptive) neurons in the DRG were spared from apoptosis in Wnt1-cKO mice, in agreement with previous results (George et al., 2013), despite clear evidence that they do not normally innervate skeletal muscle. These results are similar to Egr3-deficient mice, which also have diminished skeletal muscle innervation by proprioceptive neurons, yet show no abnormalities in their survival (Tourtellotte and Milbrandt, 1998). Unlike TrkA+ or TrkB+ neurons, TrkC+ neurons have central processes that directly synapse on motor neurons in the spinal cord, which may provide trophic support for their survival despite impaired peripheral target innervation. Nevertheless, we found that both sensory and sympathetic Elp1-deficient neurons showed no abnormalities in survival when provided adequate neurotrophin support *in vitro*, but they had significantly attenuated neurite outgrowth and branching, similar to cortical neurons with reduced Elp1 (Creppe et al., 2009). Here too, these results differed from Hunnicutt et al. (Hunnicut et al., 2012), who showed that reduction of Elp1 in chick sensory neurons by shRNA leads to increased (not decreased) neurite branching. It is unclear whether this is a consequence of species difference or off-target shRNA effects in the chick neurons compared with genetic ablation of Elp1 in mouse neurons.

To examine whether neuron specification or differentiation was the likely explanation for abnormal neuron survival and target tissue innervation in the absence of Elp1 (George et al., 2013; Hunnicutt et al., 2012), we ablated Elp1 in phenotypically specified sympathetic neurons using DβH-iCre mice (DβH-cKO). This resulted in normal sympathetic lineage marker expression, but significant target tissue innervation abnormalities and neuron death, similar to Wnt1-cKO neurons that lacked Elp1 at earlier stages of development. Although residual sympathetic axon bundles in newborn DβH-cKO mice appeared to show decreased branching and innervation patterning in many target organs, it was not possible to clearly discriminate the extent to which axon loss may have contributed to the abnormalities. Similarly, we did not evaluate the extent to which additional sympathetic neuron autonomous abnormalities may have contributed as Elp1 could have roles in axon guidance and/or target-derived NGF retrograde transport and signaling. Taken together, our results suggest that the majority of sensory and sympathetic neuron loss in the absence of Elp1 occurs because the neurons fail to properly innervate their peripheral target tissues and to obtain adequate target-derived trophic support.

Previous studies showed that Elp1-dependent α-tubulin acetylation is necessary for cortical neuron migration and dendrite outgrowth (Creppe et al., 2009). However, we were unable to detect changes in acetylated α-tubulin (Ac-αTub) in the absence of Elp1 in agreement with previous studies (Cheishvili et al., 2011; George et al., 2013). That Elp1 may have a role in some aspects of cytoskeletal regulation was previously suggested because it is primarily localized in the cytoplasm and it facilitates cytoskeletal stress responses through Jun N-terminal kinase 1 (Jnk; Mapk8 – Mouse Genome Informatics) activation (Holmberg et al., 2002). Interestingly, we found evidence of abnormal microtubule organization that was characterized by an increase in the soluble pool of tyrosinated tubulin (Y-Tub) in the cytoplasm of Elp1-deficient neurons, similar to observations previously reported in fibroblasts from individuals with FD and fibroblasts and neuron-derived cell lines after shRNA-mediated knockdown of Elp1 (Cheishvili et al., 2011). The cytoskeletal abnormalities in cells from individuals with FD or after Elp1 knockdown were correlated with decreased expression of RE-1-silencing transcription factor (Rest) and increased expression of Stmn2/SCG10 (Mori et al., 1992). As Stmn2 is normally repressed by Rest, and it has a crucial role in MT destabilization, this regulatory axis was proposed to account for abnormal Y-Tub distribution in Elp1-depleted cells. However, we found the opposite gene expression changes in primary Elp1-deficient neurons with downregulation of Stmn2 and upregulation of Rest. Elucidation of the mechanisms by

Development (2014) 141, 2452-2461 doi:10.1242/dev.107797

which Elp1 may modulate cytoskeletal reorganization in neurons and whether the Elp1-Rest-Stmn2 regulatory axis has an important role during sensory and sympathetic neuron development will require additional detailed analysis.

There is currently no effective treatment for FD, but recent studies to identify compounds that can correct abnormal Elp1 splicing in FD may be promising as long as treatment is effective in the most disease-vulnerable neurons prior to their failed target tissue innervation and death (Axelrod et al., 2011). A better mechanistic understanding of Elp1 function in disease-vulnerable neurons may elucidate new pathways that can be specifically targeted to compensate for its loss in FD.

MATERIALS AND METHODS

Animals

Elp1-flx mice were generated using homologous recombination in *E. coli* (see methods in the supplementary material). DβH-iCre PAC transgenic mice were obtained from G. Schutz (Parlato et al., 2007) and backcrossed at least five generations to the C57/BL6 genetic background. Isogenic C57BL/6J CAG-FlpE mice were obtained from the RIKEN animal resource (#RBRC01834) (Kanki et al., 2006), and Rosa26-lacZ (R26R) Cre-recombinase reporter mice (Soriano, 1999) (JAX# 003309), StLa Cre-recombinase reporter mice (Nam and Benezra, 2009) (JAX# 010633) and Wnt1-Cre transgenic driver mice (Danielian et al., 1998) (JAX# 003829) were obtained from Jackson Labs (Bar Harbor, Maine).

All mice were genotyped by PCR using genomic DNA isolated from tail biopsy tissue. For sequences of the genotyping primers and PCR conditions, see methods in the supplementary material. All experimental procedures involving mice complied with the Public Health Service Policy on Humane Care and Use of Laboratory Animals and all animal-related protocols were approved by the Northwestern University Institutional Animal Care and Use Committee (IACUC).

Tissue preparation

Anesthetized P0 mice were perfused through the heart with 0.1M phosphate-buffered (pH=7.4) 4% paraformaldehyde (PFA) and tissues were post-fixed at 4°C for 1-4 hours. Embryonic tissues were immersion fixed in PFA overnight at 4°C. For frozen sections, tissues were cryoprotected overnight at 4°C in graded (15-30%) phosphate-buffered (pH=7.4) sucrose and embedded in OCT. For quantitative studies involving cell counting of immunolabeled neurons, PFA-fixed tissues were embedded in paraffin and sectioned at 4-7 µm or frozen sections were cut at 20 µm. In some experiments, tissues were isolated fresh for RNA and/or protein extraction. *lacZ* histochemistry was performed as previously described (Eldredge et al., 2008).

Gene expression analysis

Reverse transcriptase (RT)-PCR and qPCR were performed as previously (Albert et al., 2005; Quach et al., 2013) and are outlined in detail in supplementary methods (see supplementary material).

Immunohistochemistry and western blotting

Immunohistochemistry and western blotting were performed as described previously described (Gao et al., 2007) and outlined in detail in the supplementary methods (see supplementary material).

In vivo ganglion neuron counts and primary neuron culture and cell survival

Neuron counts and primary neuron culture were performed as previously described (Quach et al., 2013). Primary neuron survival was performed as previously described and detailed as previously described (Eldredge et al., 2008).

Whole-mount TH immunohistochemistry

Whole mount TH immunohistochemistry was performed as previously described (Li et al., 2011) but with slight modification (see methods in the supplementary material).

In vivo semi-quantitative sensory and sympathetic target innervation and axon bundle branching

Quantification of target tissue innervation on tissue sections from newborn Wnt-1-Cre^{+};Elp1$^{+/+}$ (Wnt1-Ctl), DβH-iCre^{+};Elp1$^{+/+}$ (DβH-Ctl), Wnt-1-Cre^{+};Elp1$^{f/f}$ (Wnt1-cKO) and DβH-iCre^{+};Elp1$^{f/f}$ (DβH-cKO) mice was performed using fluorescence densitometry. Fluorescent images were captured with a Zeiss LS510 confocal microscope using identical aperture and photomultiplier tube voltage settings to ensure accurate comparison between tissues across multiple sections within and across genotypes. The density of Prph-, NF-H- and TH-positive axons and terminals was calculated using Metamorph software (Molecular Devices) as the total fluorescence intensity in a defined area (total fluorescence/area) and averaged for six separate confocal areas per section per mouse (see methods in the supplementary material).

Statistical measurements

All values were expressed as mean±s.e.m. and when individual groups were compared, Student's *t*-test was used to compare the means. In some cases, data were analyzed using repeated measures ANOVA with genotype or treatment effect as the grouping variable. In all instances, $P<0.05$ was considered statistically significant.

Acknowledgements

We thank M. Senagolage and L. Li in the Tourtellotte lab for technical assistance. Dr A. Chariot generously provided the mouse Elp1a, mouse Elp1b, shScramble and human Elp1 shRNA expression plasmids. We thank Dr S. Slaugenhaupt for her helpful advice and for providing antibodies to Elp1.

Competing interests

The authors declare no competing financial interests.

Author contributions

M.Z.J. and W.G.T. designed the research, performed experiments and wrote the paper. K.A.G. and C.Q. performed some experiments.

Funding

This work was supported by National Institutes of Health (NIH) grants [R21-HD063078, K02-NS046468 and K26-OD026099 (to W.G.T.)]. M.Z.J. was supported by the NIH [F31-NS071942]. Deposited in PMC for release after 12 months.

Supplementary material

Supplementary material available online at
http://dev.biologists.org/lookup/suppl/doi:10.1242/dev.107797/-/DC1

References

Albert, Y., Whitehead, J., Eldredge, L., Carter, J., Gao, X. and Tourtellotte, W. G. (2005). Transcriptional regulation of myotube fate specification and intrafusal muscle fiber morphogenesis. *J. Cell Biol.* **169**, 257-268.

Anderson, S. L., Coli, R., Daly, I. W., Kichula, E. A., Rork, M. J., Volpi, S. A., Ekstein, J. and Rubin, B. Y. (2001). Familial dysautonomia is caused by mutations of the IKAP gene. *Am. J. Hum. Genet.* **68**, 753-758.

Axelrod, F. B. (2004). Familial dysautonomia. *Muscle Nerve* **29**, 352-363.

Axelrod, F. B. and Gold-von Simson, G. (2007). Hereditary sensory and autonomic neuropathies: types II, III, and IV. *Orphanet J. Rare Dis.* **2**, 39.

Axelrod, F. B., Iyer, K., Fish, I., Pearson, J., Sein, M. E. and Spielholz, N. (1981). Progressive sensory loss in familial dysautonomia. *Pediatrics* **67**, 517-522.

Axelrod, F. B., Liebes, L., Gold-von Simson, G., Mendoza, S., Mull, J., Leyne, M., Norcliffe-Kaufmann, L., Kaufmann, H. and Slaugenhaupt, S. A. (2011). Kinetin improves IKBKAP mRNA splicing in patients with familial dysautonomia. *Pediatr. Res.* **70**, 480-483.

Cheishvili, D., Maayan, C., Smith, Y., Ast, G. and Razin, A. (2007). IKAP/hELP1 deficiency in the cerebrum of familial dysautonomia patients results in down regulation of genes involved in oligodendrocyte differentiation and in myelination. *Hum. Mol. Genet.* **16**, 2097-2104.

Cheishvili, D., Maayan, C., Cohen-Kupiec, R., Lefler, S., Weil, M., Ast, G. and Razin, A. (2011). IKAP/Elp1 involvement in cytoskeleton regulation and implication for familial dysautonomia. *Hum. Mol. Genet.* **20**, 1585-1594.

Chen, Y.-T., Hims, M. M., Shetty, R. S., Mull, J., Liu, L., Leyne, M. and Slaugenhaupt, S. A. (2009). Loss of mouse Ikbkap, a subunit of elongator, leads to transcriptional deficits and embryonic lethality that can be rescued by human IKBKAP. *Mol. Cell. Biol.* **29**, 736-744.

Close, P., Hawkes, N., Cornez, I., Creppe, C., Lambert, C. A., Rogister, B., Siebenlist, U., Merville, M.-P., Slaugenhaupt, S. A., Bours, V. et al. (2006).

Transcription impairment and cell migration defects in elongator-depleted cells: implication for familial dysautonomia. *Mol. Cell* **22**, 521-531.

Cohen-Kupiec, R., Pasmanik-Chor, M., Oron-Karni, V. and Weil, M. (2011). Effects of IKAP/hELP1 deficiency on gene expression in differentiating neuroblastoma cells: implications for familial dysautonomia. *PLoS ONE* **6**, e19147.

Cordero, D. R., Brugmann, S., Chu, Y., Bajpai, R., Jame, M. and Helms, J. A. (2011). Cranial neural crest cells on the move: their roles in craniofacial development. *Am. J. Med. Genet. A* **155**, 270-279.

Creppe, C., Malinouskaya, L., Volvert, M. L., Gillard, M., Close, P., Malaise, O., Laguesse, S., Cornez, I., Rahmouni, S., Ormenese, S. et al. (2009). Elongator controls the migration and differentiation of cortical neurons through acetylation of alpha-tubulin. *Cell* **136**, 551-564.

Cuajungco, M. P., Leyne, M., Mull, J., Gill, S. P., Lu, W., Zagzag, D., Axelrod, F. B., Maayan, C., Gusella, J. F. and Slaugenhaupt, S. A. (2003). Tissue-specific reduction in splicing efficiency of IKBKAP due to the major mutation associated with familial dysautonomia. *Am. J. Hum. Genet.* **72**, 749-758.

Danielian, P. S., Muccino, D., Rowitch, D. H., Michael, S. K. and McMahon, A. P. (1998). Modification of gene activity in mouse embryos in utero by a tamoxifen-inducible form of Cre recombinase. *Curr. Biol.* **8**, 1323-1326.

Dietrich, P., Yue, J., E, S. and Dragatsis, I. (2011). Deletion of exon 20 of the Familial Dysautonomia gene Ikbkap in mice causes developmental delay, cardiovascular defects, and early embryonic lethality. *PLoS ONE* **6**, e27015.

Eldredge, L. C., Gao, X. M., Quach, D. H., Li, L., Han, X., Lomasney, J. and Tourtellotte, W. G. (2008). Abnormal sympathetic nervous system development, physiological dysautonomia in Egr3-deficient mice. *Development* **135**, 2949-2957.

Gao, X., Daugherty, R. L. and Tourtellotte, W. G. (2007). Regulation of low affinity neurotrophin receptor (p75NTR) by early growth response (Egr) transcriptional regulators. *Mol. Cell. Neurosci.* **36**, 501-514.

George, L., Chaverra, M., Wolfe, L., Thorne, J., Close-Davis, M., Eibs, A., Riojas, V., Grindeland, A., Orr, M., Carlson, G. A. et al. (2013). Familial dysautonomia model reveals Ikbkap deletion causes apoptosis of Pax3+ progenitors and peripheral neurons. *Proc. Natl. Acad. Sci. U.S.A.* **110**, 18698-18703.

Hart, A. W., Morgan, J. E., Schneider, J., West, K., McKie, L., Bhattacharya, S., Jackson, I. J. and Cross, S. H. (2006). Cardiac malformations and midline skeletal defects in mice lacking filamin A. *Hum. Mol. Genet.* **15**, 2457-2467.

Holmberg, C., Katz, S., Lerdrup, M., Herdegen, T., Jäättelä, M., Aronheim, A. and Kallunki, T. (2002). A novel specific role for I kappa B kinase complex-associated protein in cytosolic stress signaling. *J. Biol. Chem.* **277**, 31918-31928.

Honma, Y., Kawano, M., Kohsaka, S. and Ogawa, M. (2010). Axonal projections of mechanoreceptive dorsal root ganglion neurons depend on Ret. *Development* **137**, 2319-2328.

Hunnicutt, B. J., Chaverra, M., George, L. and Lefcort, F. (2012). IKAP/Elp1 is required in vivo for neurogenesis and neuronal survival, but not for neural crest migration. *PLoS ONE* **7**, e32050.

Johansen, L. D., Naumanen, T., Knudsen, A., Westerlund, N., Gromova, I., Junttila, M., Nielsen, C., Bottzauw, T., Tolkovsky, A., Westermarck, J. et al. (2008). IKAP localizes to membrane ruffles with filamin A and regulates actin cytoskeleton organization and cell migration. *J. Cell Sci.* **121**, 854-864.

Kanki, H., Suzuki, H. and Itohara, S. (2006). High-efficiency CAG-FLPe deleter mice in C57BL/6J background. *Exp. Anim.* **55**, 137-141.

Lee, G., Papapetrou, E. P., Kim, H., Chambers, S. M., Tomishima, M. J., Fasano, C. A., Ganat, Y. M., Menon, J., Shimizu, F., Viale, A. et al. (2009). Modelling pathogenesis and treatment of familial dysautonomia using patient-specific iPSCs. *Nature* **461**, 402-406.

Lehavi, O., Aizenstein, O., Bercovich, D., Pavzner, D., Shomrat, R., Orr-Urtreger, A. and Yaron, Y. (2003). Screening for familial dysautonomia in Israel: evidence for higher carrier rate among Polish Ashkenazi Jews. *Genet. Test.* **7**, 139-142.

Li, L., Eldredge, L. C., Quach, D. H., Honasoge, A., Gruner, K. and Tourtellotte, W. G. (2011). Egr3 dependent sympathetic target tissue innervation in the absence of neuron death. *PLoS One* **6**, e25696.

Liu, P., Jenkins, N. A. and Copeland, N. G. (2003). A highly efficient recombineering-based method for generating conditional knockout mutations. *Genome Res.* **13**, 476-484.

Maayan, C., Kaplan, E., Shachar, S., Peleg, O. and Godfrey, S. (1987). Incidence of familial dysautonomia in Israel 1977-1981. *Clin. Genet.* **32**, 106-108.

Magin, T. M., McWhir, J. and Melton, D. W. (1992). A new mouse embryonic stem cell line with good germ line contribution and gene targeting frequency. *Nucleic Acids Res.* **20**, 3795-3796.

Mass, E., Brin, I., Belostoky, L., Maayan, C. and Gadoth, N. (1998). A cephalometric evaluation of craniofacial morphology in familial dysautonomia. *Cleft Palate Craniofac. J.* **35**, 120-126.

Mori, N. and Morii, H. (2002). SCG10-related neuronal growth-associated proteins in neural development, plasticity, degeneration, and aging. *J. Neurosci. Res.* **70**, 264-273.

Mori, N., Schoenherr, C., Vandenbergh, D. J. and Anderson, D. J. (1992). A common silencer element in the SCG10 and type II Na+ channel genes binds a factor present in nonneuronal cells but not in neuronal cells. *Neuron* **9**, 45-54.

Murphy, M., Reid, K., Brown, M. A. and Bartlett, P. F. (1993). Involvement of leukemia inhibitory factor and nerve growth factor in the development of dorsal root ganglion neurons. *Development* **117**, 1173-1182.

Nam, H.-S. and Benezra, R. (2009). High levels of Id1 expression define B1 type adult neural stem cells. *Cell Stem Cell* **5**, 515-526.

Naumanen, T., Johansen, L. D., Coffey, E. T. and Kallunki, T. (2008). Loss-of-function of IKAP/ELP1: could neuronal migration defect underlie familial dysautonomia? *Cell Adh. Migr.* **2**, 236-239.

Otero, G., Fellows, J., Li, Y., de Bizemont, T., Dirac, A. M. G., Gustafsson, C. M., Erdjument-Bromage, H., Tempst, P. and Svejstrup, J. Q. (1999). Elongator, a multisubunit component of a novel RNA polymerase II holoenzyme for transcriptional elongation. *Mol. Cell* **3**, 109-118.

Parlato, R., Otto, C., Begus, Y., Stotz, S. and Schutz, G. (2007). Specific ablation of the transcription factor CREB in sympathetic neurons surprisingly protects against developmentally regulated apoptosis. *Development* **134**, 1663-1670.

Pearson, J. and Pytel, B. A. (1978). Quantitative studies of sympathetic ganglia and spinal cord intermedio-lateral gray columns in familial dysautonomia. *J. Neurol. Sci.* **39**, 47-59.

Pearson, J., Pytel, B. A., Grover-Johnson, N., Axelrod, F. and Dancis, J. (1978). Quantitative studies of dorsal root ganglia and neuropathologic observations on spinal cords in familial dysautonomia. *J. Neurol. Sci.* **35**, 77-92.

Quach, D. H., Oliveira-Fernandes, M., Gruner, K. A. and Tourtellotte, W. G. (2013). A sympathetic neuron autonomous role for Egr3-mediated gene regulation in dendrite morphogenesis and target tissue innervation. *J. Neurosci.* **33**, 4570-4583.

Raible, D. W. and Ungos, J. M. (2006). Specification of sensory neuron cell fate from the neural crest. *Adv. Exp. Med. Biol.* **589**, 170-180.

Rohrer, H. (2011). Transcriptional control of differentiation and neurogenesis in autonomic ganglia. *Eur. J. Neurosci.* **34**, 1563-1573.

Rotthier, A., Baets, J., De Vriendt, E., Jacobs, A., Auer-Grumbach, M., Lévy, N., Bonello-Palot, N., Kilic, S. S., Weis, J., Nascimento, A. et al. (2009). Genes for hereditary sensory and autonomic neuropathies: a genotype-phenotype correlation. *Brain* **132**, 2699-2711.

Rotthier, A., Baets, J., Timmerman, V. and Janssens, K. (2012). Mechanisms of disease in hereditary sensory and autonomic neuropathies. *Nat. Rev. Neurol.* **8**, 73-85.

Serbedzija, G. N., Fraser, S. E. and Bronner-Fraser, M. (1990). Pathways of trunk neural crest cell migration in the mouse embryo as revealed by vital dye labelling. *Development* **108**, 605-612.

Slaugenhaupt, S. A., Blumenfeld, A., Gill, S. P., Leyne, M., Mull, J., Cuajungco, M. P., Liebert, C. B., Chadwick, B., Idelson, M., Reznik, L. et al. (2001). Tissue-specific expression of a splicing mutation in the IKBKAP gene causes familial dysautonomia. *Am. J. Hum. Genet.* **68**, 598-605.

Solinger, J. A., Paolinelli, R., Klöß, H., Scorza, F. B., Marchesi, S., Sauder, U., Mitsushima, D., Capuani, F., Stürzenbaum, S. R. and Cassata, G. (2010). The Caenorhabditis elegans Elongator complex regulates neuronal alpha-tubulin acetylation. *PLoS Genet.* **6**, e1000820.

Soriano, P. (1999). Generalized lacZ expression with the ROSA26 Cre reporter strain. *Nat. Genet.* **21**, 70-71.

Sylvie, J., Ellen, C. and Kris, V. (2011). The role of Wnt in cell signaling and cell adhesion during early vertebrate development. *Front. Biosci. (Landmark Ed)* **16**, 2352-2366.

Tourtellotte, W. G. and Milbrandt, J. (1998). Sensory ataxia and muscle spindle agenesis in mice lacking the transcription factor Egr3. *Nat. Genet.* **20**, 87-91.

Tourtellotte, W. G., Keller-Peck, C., Milbrandt, J. and Kucera, J. (2001). The transcription factor Egr3 modulates sensory axon-myotube interactions during muscle spindle morphogenesis. *Dev. Biol.* **232**, 388-399.